

Optimized Robotic Grippers Based on Scissor-like Elements

Tiancheng Gao

School of Future Aerospace Technology, Beihang University, Beijing, 100191, China

Gordon200309@outlook.com

Abstract. The grippers are the decisive part of the robot palletizer and the structure of the grippers is the decisive factor of the ability of robot palletizers to grab targets in different shapes. Inspired by scissor-like elements, an optimized rigid structure of robotic grippers based on the two-dimensional pantograph is proposed which has 1 degree of freedom and can move without strain. The path of the movement of the grippers is easy to be calculated and controlled and due to the design of the hydraulics, each finger of the grippers can move separately when powered by only one motor which can better fit the shape of the targets to grab them more tightly. The report includes the virtual model and kinematic analysis of the optimized robotic grippers.

Keywords: Robotic grippers, Scissor-like elements, Two-dimensional pantograph, Kinematic analysis, Hydraulics.

1 Introduction

Robotic arm has a wide range of use in various fields such as manufacturing, agriculture and etc. It can automatically and continuously accomplish different tasks especially those are repeated or hard for humans. For the robotic arms that are designed to grab and move targets known as robot palletizers, the design of their grippers is a critical factor in their function to grab targets in different shapes such as cube, cylinder, sphere and even irregular shape.

Deployable structures such as Bennett linkages, scissor-like elements and origami structures have been widely used in many fields such as medical field[1], architecture[2, 3], space science[4, 5] and the design of robots[6, 7]. Its shape can switch automatically under the power of the electric motors. So when it is applied to robotic grippers, it enables them to change structure to fit the shape of the targets better in order to hold the targets tighter. There are lots of successful applications of deployable structures in the design of the robotic grippers such as the research developed by S. Li's team[8], A. Firouzeh and J. Paik's research[9] and Z. Zhakypov's team[10]. They applied origami structures to making a soft robotic grippers that can switch their shapes. But the soft grippers require strong materials and they are hard to be powered by motors. However, the rigid deployable structures have simpler movement and can be easily driven by motors. What's more, it has less deformation than soft structures under pressure which means it can bear more weight when being used as grippers. The research developed by K. Lee's team[11] showed a successful use of origami twisted tower in building a robotic grippers which can hold targets in different shapes under the power of only one motor. But its structure is complicated and all the fingers of the grippers move simultaneously, which means that for some shapes like a cuboid whose length and width have a huge difference. The

grippers built by C. Liu's team[12] and A. Orlofsky's team[13] have the similar Miura deployable structure. Their designs are less complex than the one of K. Lee's team[11], which makes them easier to control. But the fingers of their grippers can not move separately under the power of one motor either. In this report, a practicable design of robotic grippers using deployable structures whose fingers can move separately is introduced.

The research developed by Agostino Zanardo[14] about the two dimensional articulated systems explained the geometry and kinematics of the articulated systems when rods' length and the position of the hinges vary which are similar to the scissor-like elements. Based on the scissor-like elements, Z.You[15] developed a pantograph structure which can be folded without strain. This feature indicates that it can be folded or deployed with little deformation, which makes it be able to be applied on the robotic grippers to expand, contract and carry objects.

Figure 1[15] shows three basic elements with their length factors which can build a simple two-dimensional pantograph. Element (a) and (b) is similar to each other which are both symmetric about the central line and the ratio of the length of the rods of (a) and (b) is k . Element (c) is homothetic about its joint and the ratio of the length of the left side and the right side is also k .

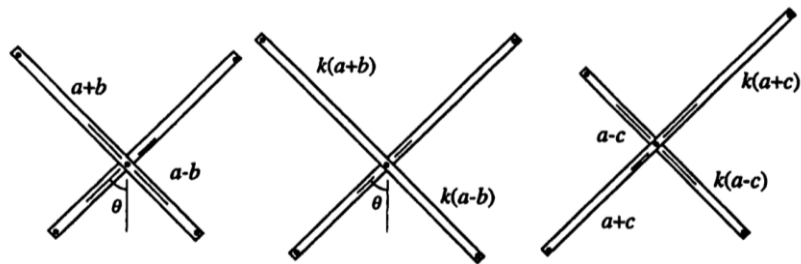


Fig. 1. (a-c) Three elements of the two-dimensional pantograph[15]

Connecting the three basic elements in the sequence (a), (c), and (b) to build a simple two-dimensional pantograph and using SOLIDWORKS to build its virtual model which is shown in Figure 2.

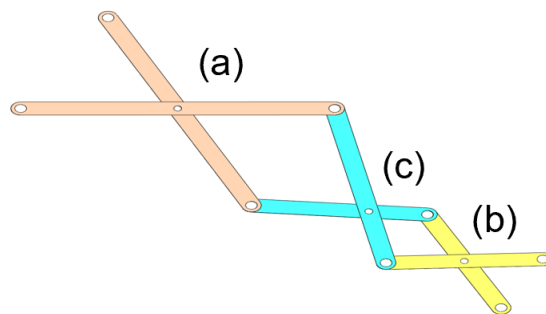


Fig. 2. A simple two-dimensional pantograph

2 The design of the unit of the gripper

To make the two-dimensional pantograph structure better fits the shape of the grippers, element (a) and (b) are cut in half and one rod of element (b) is extended. The model of the structure after being optimized can be used as the basic unit of the grippers and it is shown in the Figure 3.

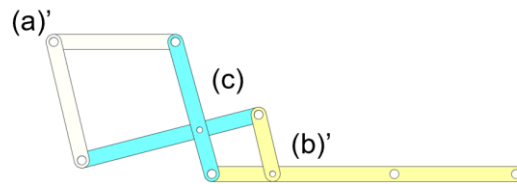


Fig. 3. The basic unit of the grippers

Adding designations to each joints and marking the length of each rods, the marked model is shown in Figure 4.

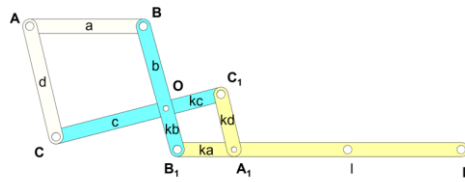


Fig. 4. The basic unit of the grippers (marked)

Once rod AB is fixed, the whole structure will expand and contract when rod AC revolves around the joint A. The different shapes of the basic unit when it is closed, half deployed and fully deployed are shown in Figure 5, 6 and 7.

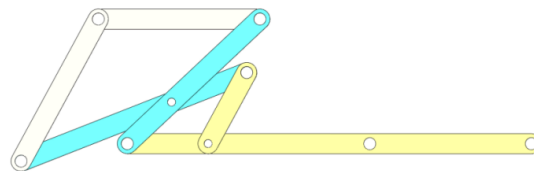


Fig. 5. The basic unit of the grippers (closed)

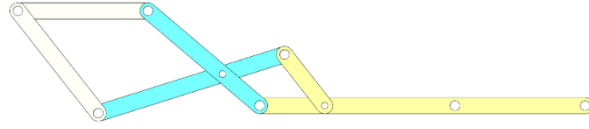


Fig. 6. The basic unit of the grippers (half deployed)

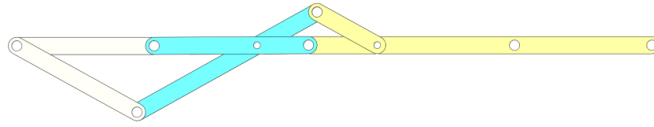


Fig. 7. The basic unit of the grippers (fully deployed)

3 Geometric and kinematic analysis

3.1 Geometric analysis

The diagram of the basic unit is shown in Figure 8. The length of each rod is in accord with the two-dimensional pantograph.

Apparently,

$$\frac{B_1O}{BO} = \frac{C_1O}{CO} = k$$

$$\angle BOC = \angle B_1OC_1 \quad (1)$$

Thus,

$$\Delta BOC \sim \Delta B_1OC_1 \quad (2)$$

Then,

$$\frac{B_1C_1}{BC} = \frac{B_1O}{BO} = k \quad (3)$$

Thus,

$$\frac{A_1B_1}{AB} = \frac{B_1C_1}{BC} = \frac{A_1C_1}{AC} = k$$

$$\Delta ABC \sim \Delta A_1B_1C_1$$

$$\angle ABC = \angle A_1B_1C_1 \quad (4)$$

Plus,

$$\angle BOC = \angle B_1OC_1 \quad (5)$$

Then,

$$\begin{aligned} \angle ABC + \angle BOC &= \angle A_1B_1C_1 + \angle B_1OC_1 \\ \angle ABO &= \angle A_1B_1O \\ A_1B_1 & // AB \end{aligned} \quad (6)$$

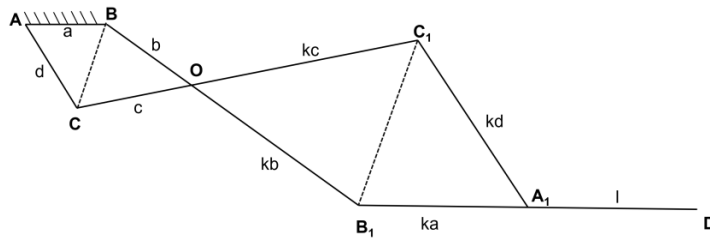


Fig. 8. Diagram of the basic unit of the grippers

According to the geometric analysis, rod A_1B_1 is always parallel to rod AB when rod AC revolves around joint A . While rod BB_1 revolves around the joint B , joint B_1 moves on a circle whose center is B and radius is $(k+1)b$. Thus, combining rod A_1B_1 is always parallel to AB , every point on line A_1B_1 moves on a circle whose center is on line AB and radius is $(k+1)b$, which is shown visually in Figure 9.

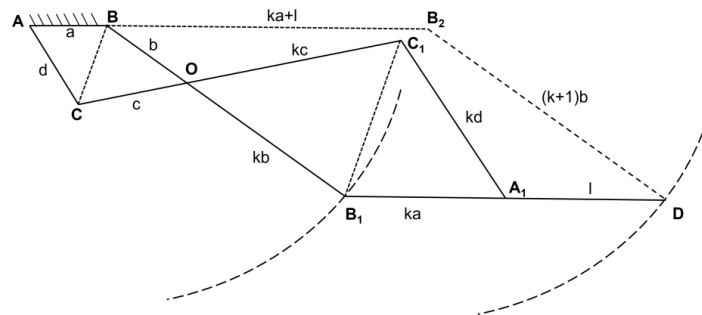


Fig. 9. Diagram of the basic unit of the grippers (with path of B_1 and D)

3.2 Kinematic analysis

The basic unit of the grippers consists of two similar four-bar linkages which are connected to each other. The amount of links except for ground (rod AB) is 5, and it has 7 revolute joints each of which have one degree of rotation freedom. Thus, once rod AB is fixed as the ground the total degree of freedom of the basic unit can be calculated by Kutzbach criterion as follows:

$$M = 3 \times (6 - 1) - 7 \times (3 - 1) = 1 \quad (7)$$

The structure has one degree of freedom and if representing the angular velocity of AC as the known input, the movement of the structure will be definite.

Another diagram of the basic unit with the specific angles marked is shown as Figure 10. One sides of θ_2 is parallel to the x-axis and the same as θ_3 and θ_4 .

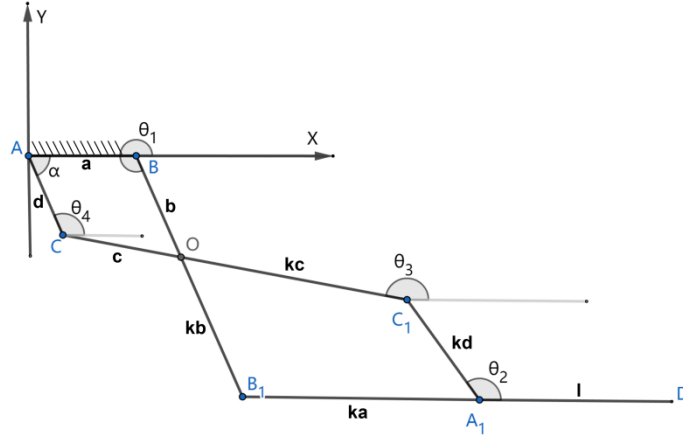


Fig. 10. Diagram of the basic unit of the grippers (with marked angles)

Representing the degree of α as the known input and the degrees of θ_1 , θ_2 , θ_3 and θ_4 are the output. The sides of θ_2 are parallel to those of θ_4 , thus $\theta_2 = \theta_4$. Then geometrically there are:

$$\begin{aligned} \theta_1 &= 360^\circ - \alpha \\ \theta_2 &= \theta_4 = 180^\circ - \alpha \end{aligned} \quad (8)$$

Following the sequence of joints A-B-B₁-A₁-C₁-C-A to form a closed loop, the loop closure equation will be:

$$ae^{j \cdot 0} + (k+1)be^{j\theta_1} + kae^{j \cdot 0} + kde^{j\theta_2} + (k+1)ce^{j\theta_3} + de^{j\theta_4} = 0 \quad (9)$$

Simplifying the loop closure equation, and considering $\theta_2 = \theta_4$, we can get the position equation of the basic unit:

$$a + be^{j\theta_1} + de^{j\theta_2} + ce^{j\theta_3} = 0 \quad (10)$$

Differentiating the position equation, we can get the velocity equation and the acceleration equation:

Velocity equation:

$$b\dot{\theta}_1 e^{j\theta_1} + d\dot{\theta}_2 e^{j\theta_2} + c\dot{\theta}_3 e^{j\theta_3} = 0 \quad (11)$$

Acceleration equation:

$$be^{j\theta_1}(\ddot{\theta}_1 + j\dot{\theta}_1^2) + de^{j\theta_2}(\ddot{\theta}_2 + j\dot{\theta}_2^2) + ce^{j\theta_3}(\ddot{\theta}_3 + j\dot{\theta}_3^2) = 0 \quad (12)$$

Considering the position equation to work out the degree of θ_1 , θ_2 , θ_3 and θ_4 as the dependent variables while the degree of α is the input, its real and imaginary parts are as follows:

Real part:

$$a + b \cos \theta_1 + d \cos \theta_2 + c \cos \theta_3 = 0 \quad (13)$$

Imaginary part:

$$b \sin \theta_1 + d \sin \theta_2 + c \sin \theta_3 = 0 \quad (14)$$

Combining with the geometric equations, there is a set of equations which has 4 variable and 4 independent equations about the degree of α , θ_1 , θ_2 , θ_3 and θ_4 :

$$\begin{cases} a + b \cos \theta_1 + d \cos \theta_2 + c \cos \theta_3 = 0 \\ b \sin \theta_1 + d \sin \theta_2 + c \sin \theta_3 = 0 \\ \theta_2 = 180^\circ - \alpha \\ \theta_4 = 180^\circ - \alpha \end{cases} \quad (15)$$

Representing $a=40\text{mm}$, $b=30\text{mm}$, $c=40\text{mm}$, $d=40\text{mm}$, which is equivalent to the length of the rods of the virtual model. Through MATLAB program, the degree of θ_1 , θ_2 , θ_3 and θ_4 as the dependent variables while the degree of α is the input is shown in the plot in Figure 11.

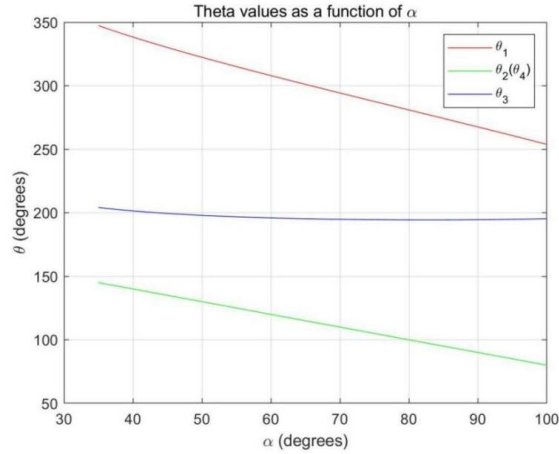


Fig. 11. Plot of the degree of θ_1 , θ_2 , θ_3 and θ_4 with α as the input

To figure out the range of movement of the rod A_1B_1 which is at the end of the grippers and is used to hold targets, mark the distance between rod A_1B_1 and AB which is on the base of the grippers as h , and the new diagram of the basic unit is shown in Figure 12.

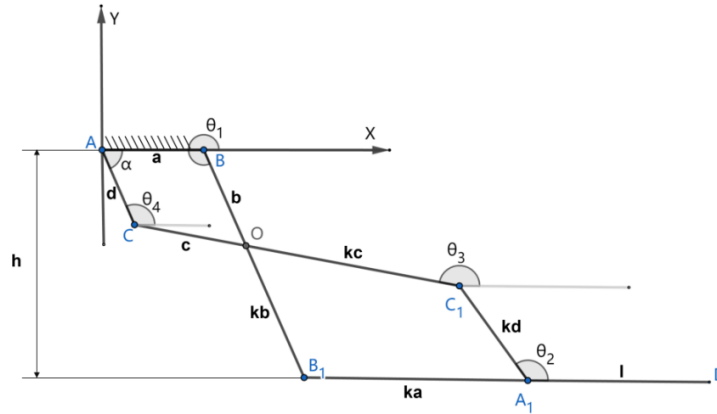


Fig. 12. Diagram of the basic unit (with marked distance h)

Geometrically,

$$h = (k + 1)b \quad (16)$$

Representing $k=2$, which is equivalent to the virtual model, and the plot of h as the dependent variable with the degree of α as the input is shown in Figure 13.

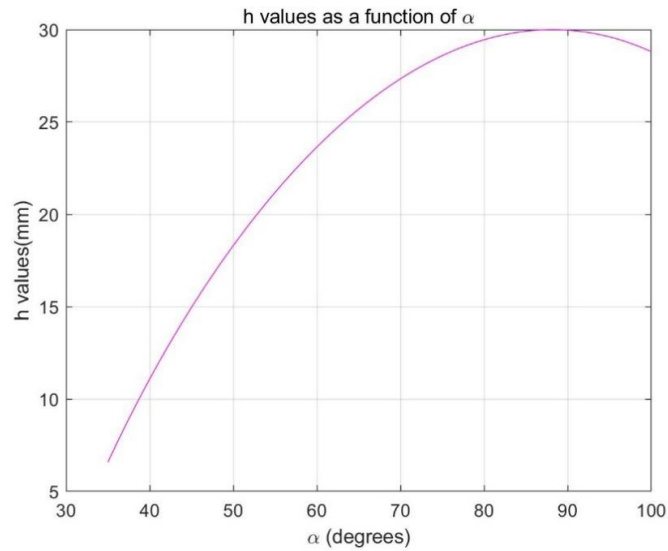


Fig. 13. Plot of h with α as the input

4 Prototype and the features

4.1 Prototype

Cutting out the rod AB and fixing the other part of the basic unit to the base of the grippers, the shape of the completed virtual model of the robotic grippers which is built in SOLIDWORKS when it is closed, half deployed and fully deployed is shown in Figure 14,15 and 16.

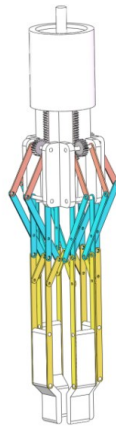


Fig. 14. The model of the robotic grippers (closed)

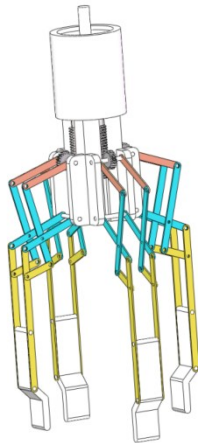


Fig. 15. The model of the robotic grippers (half deployed)

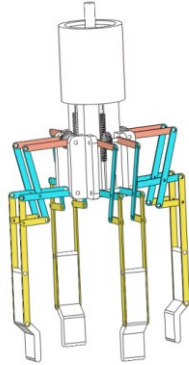


Fig. 16. The model of the robotic grippers (fully deployed)

During the whole process of its movement, the four ‘fingers’ of the grippers is always parallel to the lines on which the two joints of each finger that connect the finger to the base lie on, which makes the path of movement of each finger is easy to be calculated and controlled.

4.2 The transmission system

The transmission system the grippers consists of two critical parts. The first is the hydraulics which is shown in the Figure 17. It consists of 1 large cylinder, 4 small cylinders, and 5 plungers which fit the diameter of the 5 cylinders. There is a cavity between the large plunger and the 4 small plungers. Once the cavity is filled with water, oil or other liquids, it can transmit power of the motor which drives the large plunger to move up and down separately to the four small plungers. For liquids are difficult to compress and have no definite shapes, when one of the small plungers is forced to stop, others will continue to move under the power of the motor while keeping the volume of the liquid a constant. The process is shown in Figure 18, in which two of the plungers is forced to stop and others continue to move down.

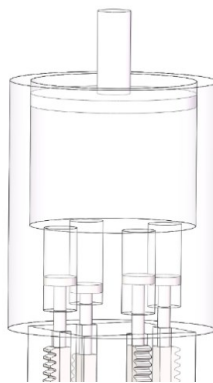


Fig. 17. The model of the hydraulics

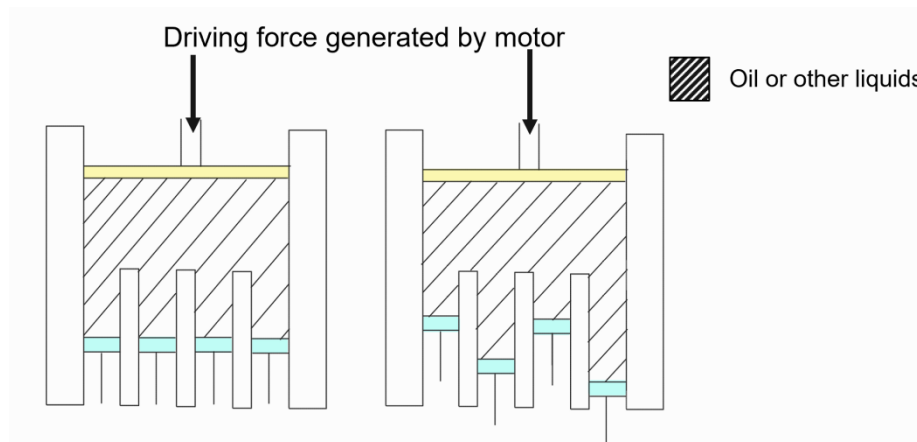


Fig. 18. The working process of the hydraulics

The second part is the rack and pinion mates that transmit the sliding of the plungers to the rotation of the pinions that are fixed to the joints of the fingers, which enable the fingers to open and close under the power of the motor. The model of the rack and pinion mates on the grippers is shown in Figure 19.

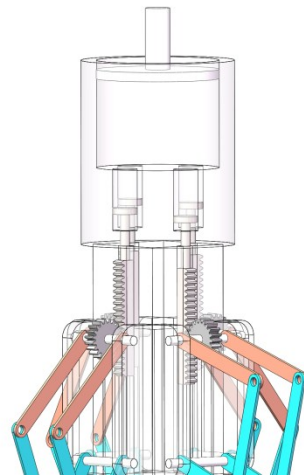


Fig. 19. The rack and pinion mates on the grippers

The transmission system allows each finger of the grippers to move separately when powered by only 1 motor. It enables the grippers to better fit the shape of the targets and reduces the failure rate causing by using more motors to separately power each finger. Once one of the fingers touches the surface of the target, it will stop moving and others will continue until all of them touch the surface of the target and the grippers grab the target tightly.

5 Discussion

The optimized robotic grippers are based on the two-dimensional pantograph and have the following features:

It can move without strain so that it can expand and contract without deformation.

Each of its unit has only 1 degree of freedom and the end of the unit is always parallel to the line which the joints of the unit that connect the unit to the base lie on. Thus, the structure has definite movement which can be easily calculated and controlled to avoid the obstacles and grab targets in the best position.

Each of its finger can move separately while it is powered by only one motor so that it can better fit the shape of the target, grab it more tightly and have higher reliability because the less motors are applied, the less possible the mechanism will break down.

6 Conclusion

This report mainly focuses on the structure of the unit of the grippers and its , transmission system. In fact there are far more factors that influence the ability of the robotic grippers such as the material applied, the kinds of the joints, the length of the rods and etc. Moreover, about the robotic grippers in this report, there are lots of parts that need to be tested and optimized: First, the grippers can be build using 3D printer and its ability to grab targets in various shapes and irregular shape along with the maximum of the weight it can bear when the targets vary need to be tested to find out if the optimized structure works well as the purpose of the research. Moreover, the structure of the basic unit needs to be tested and optimized to get better ones with better efficiency and ability to fit the shape of the targets and bear weight. And the end of the fingers in the report is a straight and rigid panel. Other material such as flexible ones and other structure of it can work better to grab the targets. There will be many interesting points about the robotic grippers to be researched and optimized in order to enhance its ability to grab different targets.

References

- [1] F. Zhang *et al.*, "Rapidly deployable and morphable 3D mesostructures with applications in multimodal biomedical devices," *Proceedings of the National Academy of Sciences*, vol. 118, no. 11, p. e2026414118, 2021.
- [2] I. Doroftei and I. A. Doroftei, "Deployable structures for architectural applications-a short review," *Applied mechanics and materials*, vol. 658, pp. 233-240, 2014.
- [3] N. De Temmerman, "Design and analysis of deployable bar structures for mobile architectural applications," 2007.
- [4] W. M. Sokolowski and S. C. Tan, "Advanced self-deployable structures for space applications," *Journal of spacecraft and rockets*, vol. 44, no. 4, pp. 750-754, 2007.
- [5] J. Santiago-Prowald and H. Baier, "Advances in deployable structures and surfaces for large apertures in space," *CEAS Space Journal*, vol. 5, pp. 89-115, 2013.
- [6] M. Askari, W. D. Shin, D. Lenherr, W. Stewart, and D. Floreano, "Avian-Inspired Claws Enable Robot Perching or Walking," *IEEE/ASME Transactions on Mechatronics*, 2023.

- [7] R. Datta, S. Pradhan, and B. Bhattacharya, "Analysis and design optimization of a robotic gripper using multiobjective genetic algorithm," *IEEE Transactions on Systems, Man, and Cybernetics: Systems*, vol. 46, no. 1, pp. 16-26, 2015.
- [8] S. Li *et al.*, "A vacuum-driven origami "magic-ball" soft gripper," in *2019 International Conference on Robotics and Automation (ICRA)*, 2019: IEEE, pp. 7401-7408.
- [9] A. Firouzeh and J. Paik, "Grasp mode and compliance control of an underactuated origami gripper using adjustable stiffness joints," *Ieee/asme Transactions on Mechatronics*, vol. 22, no. 5, pp. 2165-2173, 2017.
- [10] Z. Zhakypov, F. Heremans, A. Billard, and J. Paik, "An origami-inspired reconfigurable suction gripper for picking objects with variable shape and size," *IEEE Robotics and Automation Letters*, vol. 3, no. 4, pp. 2894-2901, 2018.
- [11] K. Lee, Y. Wang, and C. Zheng, "Twister hand: Underactuated robotic gripper inspired by origami twisted tower," *IEEE Transactions on Robotics*, vol. 36, no. 2, pp. 488-500, 2020.
- [12] C. Liu, S. J. Wohlever, M. B. Ou, T. Padir, and S. M. Felton, "Shake and take: Fast transformation of an origami gripper," *IEEE Transactions on Robotics*, vol. 38, no. 1, pp. 491-506, 2021.
- [13] A. Orlofsky, C. Liu, S. Kamrava, A. Vaziri, and S. M. Felton, "Mechanically programmed miniature origami grippers," in *2020 IEEE International Conference on Robotics and Automation (ICRA)*, 2020: IEEE, pp. 2872-2878.
- [14] A. Zanardo, "Two-dimensional articulated systems developable on a single or double curvature surface," *Meccanica*, vol. 21, pp. 106-111, 1986.
- [15] Z. You, "A pantographic deployable conic structure," *International Journal of Space Structures*, vol. 11, no. 4, pp. 363-370, 1996.

Appendix

The MATLAB codes used to calculate the degree of θ_1 , θ_2 , θ_3 and θ_4 along with the distance h is as follows.

```

clc;
clear all;

alpha = linspace(35,100,100);

a = 40;
d = 40;
c = 40;
b = 30;
k=2;

theta1_vals = zeros(1, length(alpha));
theta2_vals = zeros(1, length(alpha));
theta3_vals = zeros(1, length(alpha));
h_vals = zeros(1, length(alpha));

for i = 1:length(alpha)
    theta2 = 180 - alpha(i);

```

```

theta2_vals(i) = theta2;

fun = @(x) [
    a + b * cosd(x(1)) + d * cosd(theta2) + c * cosd(x(2));
    b * sind(x(1)) + d * sind(theta2) + c * sind(x(2))
];

x0 = [0, 0];

options = optimoptions('fsolve', 'Display', 'none');
sol = fsolve(fun, x0, options);

theta1 = sol(1);
theta3 = sol(2);

while theta1 < 0
    theta1 = theta1 + 360;
end
while theta1 > 360
    theta1 = theta1 - 360;
end

while theta3 < 0
    theta3 = theta3 + 360;
end
while theta3 > 360
    theta3 = theta3 - 360;
end

theta1_vals(i) = theta1;
theta3_vals(i) = theta3;

h_vals(i) = abs((k+1)*b * sind(theta1));
end

figure;
plot(alpha, theta1_vals, 'r');
hold on;
plot(alpha, theta2_vals, 'g');
plot(alpha, theta3_vals, 'b');
xlabel('\alpha (degrees)');
ylabel('\theta (degrees)');
legend('\theta_1', '\theta_2(\theta_4)', '\theta_3');
title('Theta values as a function of \alpha');
grid on;

figure;
plot(alpha, h_vals, 'm');

```

```
xlabel('\alpha (degrees)');  
ylabel('h values(mm)');  
title('h values as a function of \alpha');  
grid on;
```